

BIOPHYSICAL DIRECTED ASSEMBLY OF NANOSTRUCTURES FOR NEUROCOMPUTING

J.C. Wells¹, L. Maya², K. Stevenson³, T.G. Thundat³, J. Barhen¹, Y. Braiman¹, and V. Protopopescu¹

Center for Engineering Science Advanced Research

¹Computer Science and Mathematics Division

²Chemical and Analytical Sciences Division

³Life Sciences Division

Oak Ridge National Laboratory, Oak Ridge, Tennessee 37831-6355

ABSTRACT

This paper reports progress in the development of a quantum-dot array that can be operated at room temperature for carrying out nontrivial and innovative computations. We discuss the actual fabrication of 2-nm metal clusters to serve as the quantum dots, device architecture, device simulation, and the development of a computational model. Innovative and unconventional paradigms underlie the different stages of this work. For example, regular array geometry is achieved by directing appropriately derivatized metal clusters to preselected locations along a stretched strand of an engineered DNA sequence. The proposed applications include the implementation of neuromorphic algorithms for pattern recognition.

INTRODUCTION

Emerging revolutionary advances in nanoscale computing, communication, detection, and sensing, subsume a profound understanding of the complex dynamics and properties of small arrays of quantum structures, including quantum dots (QD), ultrasmall Josephson junctions, quantum-dot lasers, and others. Such arrays produce robust bi-stable and multi-stable behavior, which can be exploited for unconventional, yet powerful computational concepts, e.g., neuromorphic computing. Obtaining lattice architectures of sufficient size and regularity to perform actual computations at room temperature has been a formidable challenge, unsurmounted to date. Our objective here is to apply innovative biophysical assembly techniques to overcome this challenge. In particular, appropriately derivatized and passivated gold clusters (i.e., "quantum dots") can be directed to preselected locations along stretched strands of engineered DNA sequences to produce an operational device. Our effort includes the actual synthesis of 2-nm quantum dots, directed self-assembly of a 1D quantum-dot array via DNA templates, device simulation, and development of a computational model.

SYNTHESIS OF GOLD CLUSTERS

We have carried out the synthesis of colloidal gold clusters of core size less than 3-nm by a variety of strategies with appropriate organic coatings. A passivating coating provides a dual function. It provides a barrier for cluster growth as well as functional chemical groups for attachment to DNA nucleotides. This designed propensity for the functionalized gold cluster to bind with a nucleotide is used to assemble the nanoparticle at prescribed locations along an engineered DNA strand. Nanometer-sized metal clusters are a leading candidate for the implementation of single-electron devices at room temperature.

The strategy described here for attaching the cluster to a DNA molecule involves synthesizing gold clusters coated in hydrocarbons terminated with carboxylic-acid functionality. The carboxylic acid is made to react with thymine bases modified with amino groups (see below). Specifically, we have prepared gold colloids, which are thiol-bound to 12-carbon aliphatic hydrocarbons. This was accomplished by a procedure that involves the use of polyamido dendrimers [1], (see Fig.1). These centro-symmetric polymers act as a “nanoreactor” to confine metal ions in the cavity of the polymer. The complexed metal ions are then reduced to the charge-neutral state by means of a chemical reductant such as borohydride. In this particular case, an intermediate step is required because the dendrimer has insufficient affinity for gold ions. This step involves complexation of copper ions, which are then reduced to the metal and subjected to electroless displacement with gold ions. This displacement is feasible because gold is more noble than copper. At this point, the gold cluster must be functionalized with the carboxylic acid and the dendrimer eliminated. This is accomplished by treating an aqueous/tetrahydrofuran solution of the gold-dendrimer complex with 12-mercaptododecanoic acid and subjecting the resulting suspension to solvent extraction with toluene. The desired product, free of dendrimer, is isolated at the interface as an insoluble film, which can be solubilized in dimethylformamide. By this procedure, we have implemented the synthesis and electrophoretic separation of passivated gold clusters. Initial measurements of the cluster size distribution show a mean diameter of approximately 2 nm with a standard deviation of 30%.

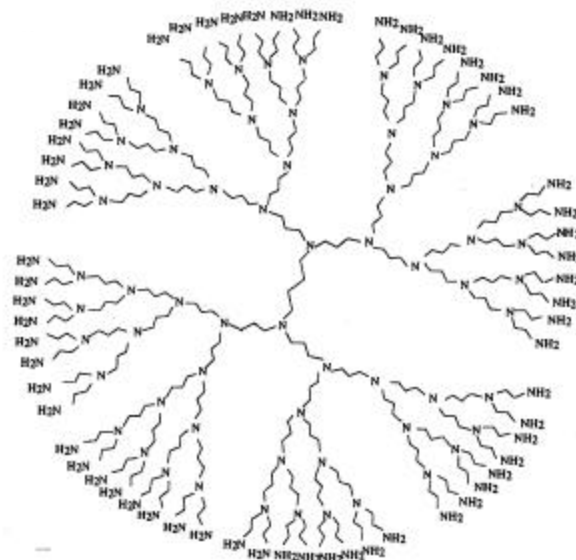


Figure 1. Polyamido dendrimers are centro-symmetric polymers that act as a “nanoreactor” in confining metal ions in cluster synthesis.

DNA TEMPLATES

The need to produce regular arrangements of nanoparticles led to the idea of using DNA as a scaffold or template for assembly of nanoscale arrays. Beginning in the 1980’s, Seeman and coworkers experimented with combining DNA fragments to produce regular geometrical shapes. To date they have succeeded in producing a variety of DNA structures, including cubes [2], triangles [3], and truncated octahedrons [4]. They have also produced two-dimensional arrays [5,6] and various forms of DNA knots [7,8]. Using DNA as a structural or template molecule has the following advantages. DNA can be synthesized using any sequence and in any length from one to several hundred nucleotides. (The length along the DNA molecule of a single nucleotide is 0.34 nm.) DNA can be joined end to end to produce longer linear molecules or more complex shapes. It can be modified at predetermined sites to allow for

the attachment of other molecules in a specific manner with subnanometer resolution. It can be cut at specific sequences and can be easily degraded when its role in assembly is complete.

Taking advantage of these properties of DNA, we have created linear arrays of DNA with binding sites located at periodic intervals for functionalized gold clusters. As a first step, we designed a single stranded DNA template with modified thymines located every 11 bases. These thymines, modified with amino groups, allow attachment of the nanoparticles at specific sites along the DNA strand through peptide bonds with carboxylic-acid functionalities (see previous section). The complementary DNA strand was synthesized and annealed to the modified strand to produce a double-stranded DNA molecule. The double-stranded DNA was then ligated to produce DNA of various lengths. Strands of the desired length can be isolated using gel electrophoresis to use for specific purposes. After ligation, the carboxyl-acid functionalized gold was bound to the amino groups on the thymine bases using 1-ethyl-3-(3-dimethylaminopropyl)carbodiimide and N-hydroxysuccinimide [9]. The DNA-gold complex was precipitated and washed, releasing the free gold. We analyzed the products using gel electrophoresis with staining for gold and using transmission electron microscopy (pictures?). In summary, we have engineered and produced DNA templates up to 200 nm long containing about 60 binding sites for gold clusters. (picture?) We are refining our procedures to ensure that every binding site along the strand is occupied with a gold cluster and that each cluster is bound to only one DNA strand. Future work will involve the extraction of a single strand of DNA with the gold and attachment to electrodes for measurements of the current-voltage (i.e., $I(V)$) characteristics of the array.

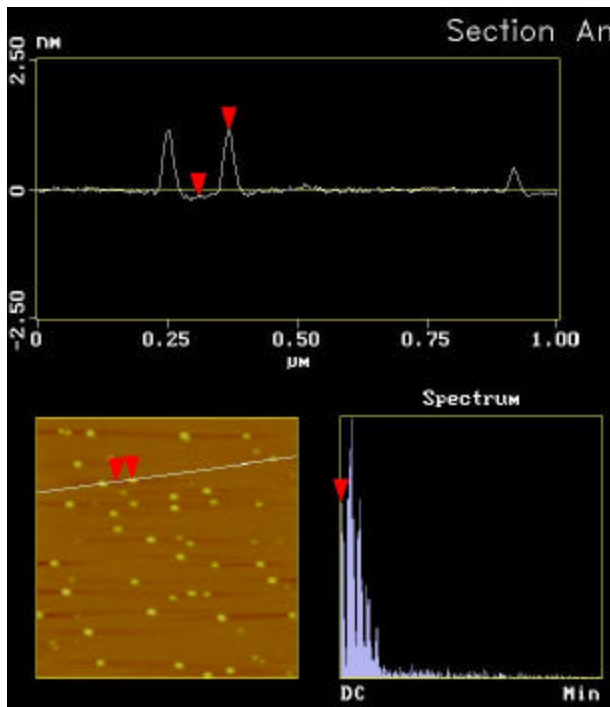


Figure 2. AFM image of gold clusters.

ELECTRODE CONSTRUCTION

Operating the QD array as an electronic device requires placing the QDs between two electrodes. This alone is a challenging task, as the electrodes are the objects that made the connection between the nanoscopic and macroscopic worlds. Using our currently available facilities, electrodes can be fabricated with separation of approximately 20 nm using a focused ion beam (FIB). In the near future, we anticipate having available an electron-beam facility for the fabrication of electrodes.

The modified DNA molecules can be stretched between the electrodes to provide electrical connectivity to the quantum-dot array [10]. A thiol group will modify one end of the DNA. A drop of DNA in solution can be placed between the electrodes using a micro-positioner. The drop size will be much larger than the gap width of the electrodes. Since the electrodes are made of gold, the thiol-modified end of DNA will attach to both gold electrodes. These anchored DNA molecules can be stretched under DNA buffer solution using hydrodynamic forces. It is also possible to use an electric field to achieve orientation of the DNA molecules between electrodes. Drying the DNA molecules can cause alterations in structure and orientation due to a variety of effects. Using the technique of critical point drying [11,12] can preserve the geometry of the stretched DNA. The resulting QD structures can be

visualized using an AFM. If more than one DNA strand is stretched between the electrodes, the AFM can be used to selectively dissect unwanted DNA strands.

The DNA strand may act as conduit for leakage currents, and should be removed, but without removing or modifying the gold clusters. One might consider heat treatment for this task, but heat treatment is likely to result in rearrangement of the quantum-dot-array geometry, and can also affect the electrodes due to diffusion. We will utilize a novel UV-Ozone technique that will chip away the DNA molecules without affecting the position of the electrodes or the clusters. The UV-Ozone technique involves exposing organic molecules (such as DNA) to 180-nm UV light. The UV light creates ozone from oxygen, which oxidizes the carbon containing molecules to carbon monoxide, which readily leaves the surface.

SINGLE-ELECTRON TUNNELING IN QUANTUM-DOT ARRAYS

Consider a one-dimensional array of N tunnel junctions constructed from metallic source and drain electrodes weakly coupled to a linear array of $N-1$ metal clusters. We review the results of the ‘‘orthodox theory’’ of single-electron tunneling [13] to describe the charge transport through the array under small, but finite, bias voltage. (We are interested in nanometer-sized metal clusters in which the Coulomb blockade of conductance may be observed at room temperature, but for simplicity here we neglect any discreteness in the density of electronic states in the cluster resulting from their small size.) The vector \vec{n} defines the state of our system, $\vec{n} \equiv (n_1, \dots, n_i, \dots, n_{N-1})$, where n_i is the number of excess electrons accommodated by the i^{th} quantum dot. The Gibbs free energy $E(\vec{n}, V)$ describing the electrostatic energy of the array of quantum dots and its interaction with the external voltage is

$$E(\vec{n}, V) = \frac{1}{2} \sum_{i=1}^{N-1} C_{ii} \mathbf{f}_i^2 + \frac{1}{2} \sum_{i=1}^N \sum_{j=0, j \neq i}^N C_{ij} (\mathbf{f}_i - \mathbf{f}_j)^2 - V_s Q_s - V_d Q_d, \quad (1.1)$$

where $C_{ij} = C_{ji}$ is the mutual capacitance between conductors i and j , \mathbf{f}_i is the electrical potential of cluster i measured with respect to the substrate. The source and drain electrodes are enumerated $i=0$ and $i=N$, respectively. The source potential is $\mathbf{f}_0 = V_s = V/2$, and the drain potential is $\mathbf{f}_N = V_d = -V/2$. V is the transport voltage across the array. The charge on the source electrode is $Q_s = C_{01}(\mathbf{f}_0 - \mathbf{f}_1) + en_s$, and the charge on the drain electrode is $Q_d = C_{N-1,N}(\mathbf{f}_N - \mathbf{f}_{N-1}) + en_d$, where n_s (n_d) is the number of electrons that has tunneled from the source (drain) electrode through the first (last) junction.

To determine the free energy, the potentials $\mathbf{f} = (\mathbf{f}_1, \dots, \mathbf{f}_{N-1})$ must be determined from the static charge configuration. Using the charge conservation law, the total charge on island i can be written in terms of the potentials,

$$q_i = C_{ii} \mathbf{f}_i + \sum_{j=0, j \neq i}^N C_{ij} (\mathbf{f}_i - \mathbf{f}_j)^2 = en_i + q_{0,i}, \quad i = 1, \dots, N-1. \quad (1.2)$$

The background charges $-e/2 < q_{0,i} < +e/2$ are due to incompletely screened charges in the environment of the islands. Equation (1.2) can be written in matrix form $\vec{Q} = \underline{C} \vec{\mathbf{f}}$, where the generalized capacitance matrix elements are defined

$$\underline{C}_{ii} \equiv \sum_{j=0}^N C_{ij}; \quad \underline{C}_{ij} = -C_{ij}, \quad (1.3)$$

and the augmented charge vector is defined $Q_i \equiv q_i + C_{i0} \mathbf{f}_0 + C_{iN} \mathbf{f}_N$. The generalized capacitance matrix can be inverted to obtain the potential distribution given any charge distribution. For convenience, we rewrite the free energy of the array using the matrix notation

$$E(\vec{n}, V) = \frac{1}{2} \vec{Q}^T \underline{C}^{-1} \vec{Q} - V_s Q_s - V_d Q_d \quad (1.4)$$

In describing the electron transport through the array, we neglect here the effects of co-tunneling, and consider only single-electron tunneling between nearest neighbors in the array. That is, the final state \vec{m} of the tunneling differs from the initial state \vec{n} by the transfer of a single electron through the k^{th} junction, e.g., $\vec{m} = \vec{n} \pm \Delta \hat{u}_k$, where $\Delta \hat{u}_k \equiv \hat{u}_k - \hat{u}_{k-1}$ and \hat{u}_k is a unit vector for the k^{th} quantum dot. The \pm sign

gives the direction of tunneling through the junction. If the transition rates are sufficiently small one can perform a calculation using Fermi's Golden Rule to obtain [13]

$$\Gamma_k^\pm(\bar{n}, V) = \Gamma_k^\pm(\Delta E_k^\pm(\bar{n}, V)) = \frac{-\Delta E_k^\pm}{e^2 R_k} \left[1 - \exp\left(\frac{\Delta E_k^\pm}{k_B T}\right) \right]^{-1} \quad (1.5)$$

where $\Delta E_k^\pm(\bar{n}, V) \equiv E(\bar{n} \pm \Delta u_k, V) - E(\bar{n}, V)$ is the change in the Gibbs free energy of the system due to the tunneling, R_k is the effective resistance of the tunnel junction, $e > 0$ is the fundamental unit of charge, and the thermal energy is $k_B T$. One can use probability conservation to write the corresponding master equation describing the time evolution of the probability $P(\bar{n}, t)$ of finding the circuit in the state \bar{n}

$$\frac{dP(\bar{n}, t)}{dt} = \sum_k \left[\Gamma_{k-1}^+(\bar{n} - \Delta \hat{u}_{k-1}) P(\bar{n} - \Delta \hat{u}_{k-1}, t) + \Gamma_k^-(\bar{n} + \Delta \hat{u}_k) P(\bar{n} + \Delta \hat{u}_k, t) \right] - \sum_{i=1}^N \left[\Gamma_k^+(\bar{n}) + \Gamma_k^-(\bar{n}) \right] P(\bar{n}, t). \quad (1.6)$$

Practical approaches to solving the master equation are described in Refs. [14-15]. Given the solution, the average tunneling current is given by the net flow through any junction k in the array:

$$I(V) = I_k(V) = e \sum_{\bar{n}} P(\bar{n}) \left[\Gamma_k^+(\bar{n}) - \Gamma_k^-(\bar{n}) \right]. \quad (1.7)$$

Since the charge states are averaged over, the current is a function of the transport voltage.

NEUROMORPHIC ALGORITHMS FOR COMPLEX INFORMATION PROCESSING

Quantum dot nanoelectronic devices represent a promising hardware technology that offers both conceptual opportunities and engineering challenges for complex information processing applications. One such application, pattern recognition, is of considerable interest to the development of modern intelligent systems and will be considered here. In recent years, the quest for innovative approaches to machine intelligence has received considerable attention. The proven ability of neuromorphic algorithms to deal with uncertain information and to interact with dynamic environments is therefore providing a strong incentive to explore the feasibility of their implementation on arrays of quantum dots. However, in contrast to conventional hardware approaches, we must develop here computational paradigms that exploit from the onset not only the concept of massive parallelism but also, and most importantly, the physics of the underlying device.

Artificial neural networks are adaptive systems that process information by means of their response to discrete or continuous input [16]. Neural networks can provide practical solutions to a variety of artificial intelligence problems, including pattern recognition [17], autonomous knowledge acquisition from observations of correlated activities [18], real-time control of complex systems [19], and fast adaptive optimization [20]. At the heart of such advances lies the development of efficient computational methodologies for "learning" [21]. The development of neural learning algorithms has generally been based upon the minimization of an energy-like neuromorphic error function or functional [22]. Gradient-based techniques have typically provided the main computational mechanism for carrying out the minimization process, often resulting in excessive training times for the large-scale networks needed to address real-life applications. Consequently, to date, considerable efforts have been devoted to: (1) speeding up the rate of convergence [23-25] and (2) designing more efficient methodologies for deriving the gradients of these functions or functionals with respect to the parameters of the network [26,27]. The primary focus of such efforts has been on recurrent architectures. However, the use of gradient methods presents challenges even for the less demanding multi-layer feed-forward architectures, which naturally occur in quantum-dot arrays. For instance, entrapment in local minima has remained one of the fundamental limitations of most currently available learning paradigms. The recent development of the innovative global optimization algorithm TRUST [28] has been suggested [29] as a promising new avenue for addressing such difficulties.

Roychowdhury and his collaborators were the first to propose the implementation of neural networks in terms of quantum dot arrays [30]. In their *Gedankenexperiment* a generic array of

nanometer-sized metallic islands would be deposited on a resonant tunneling diode. Furthermore, all islands would have a direct conductive/capacitive link to their nearest neighbors established, for example via organic molecular wires. They considered both continuous and discrete charge networks. The latter are of interest here. The Roychowdhury team showed that the evolution of an initial charge distribution toward a stable final equilibrium distribution can be given a neuromorphic interpretation and that this property emerges purely as a result of the discreteness of the electronic charge [31]. There are several shortcomings in their proposal. First, they assumed that all inter-island capacitance could be modified arbitrarily, but offered no mechanism to achieve this essential property. Moreover, their architecture involved capacitive coupling between all islands, a “floating” plate, and a grounded plate. Tunneling is assumed to occur only between the islands and the floating plate, but not between islands. Thus, even though their paradigm would allow some elementary form of combinatorial optimization, it could not be used for neural learning needed in pattern recognition.

In the previous section we have illustrated the underlying physical concepts of single-electron transport in arrays of quantum dots. As pointed out by Roychowdhury and coworkers [30-31], there is a profound similarity between the dynamics of neural networks and that of quantum-dot arrays. In the latter, the free energy of an array characterized by a distributed charge can be lowered in terms of tunneling events. For neural networks, on the other hand, Hopfield has shown that the stable states of the network are the local minima of a bounded Lyapunov function of the net’s output parametrized by the synaptic interconnection weights. A careful analysis, however, reveals that this formal similarity is not adequate for implementing learning algorithms for pattern recognition. By comparing the leading terms of the free energy in Eq. (1.4), i.e., $\frac{1}{2}Q^T C^{-1} Q$ and the Lyapunov function in a Hopfield network, i.e., $L(x, W) = -\frac{1}{2}x^T W x$, we see that the inverse of the augmented capacitance matrix would have to play the role of the synaptic matrix. However, the elements of C_{ij} are *fixed*, and cannot be modified. An alternative approach for controlling the dynamics of the system has to be found. In principle, one could manipulate the free energy of the array via capacitive gating of each of the quantum dots. However, for an array of quantum dots 1 to 2 nm in size, which is necessary for room temperature operation, we are not aware of technology capable of implementing such gating on a nanometer scale.

Studies of the dynamics of arrays of quantum dots in the presence of the time dependent excitation (such as, for example, RF signal [33,34]) reveal a rich structure of dynamical behaviors that offers a tremendous potential for performing the computation we need. In particular, a team led by Oosterkamp has recently made available an extensive survey of experiments and methods for photon-assisted tunneling in quantum dots [21]. In the absence of a time-dependent field, current flows through a quantum dot via tunneling when an unoccupied internal energy state is aligned to the Fermi energy of the leads. However, as pointed out by Oosterkamp *et al* following seminal work by Likharev *et al.*, if a time-varying AC voltage $A_0 \cos(2\pi\nu t)$ is applied, inelastic tunnel events are induced when electrons exchange photons of energy $\hbar\nu$ with the oscillating field. The tunneling rate $\bar{\Gamma}$ through each barrier in the presence of an electromagnetic excitation becomes

$$\bar{\Gamma}_k^\pm(\Delta_k^\pm E, A_0, \mathbf{n}) = \sum_{a=-\infty}^{\infty} J_a \left(\frac{eA_0}{\hbar\nu} \right) \Gamma_k^\pm(\Delta E_k^\pm + a\hbar\nu) \quad (1.8)$$

where Γ is the rate in absence of outside excitation, and J_a denotes the Bessel function of the first kind, with a denoting the number of photons exchanged and. As a result, the master equation is readily generalized to the case of external, alternating fields by substituting the rates given in Eq. (1.8) into Eq. (1.6). The current through this device can then written as a function of the transport voltage V , and the amplitude A_0 and frequency ν of the AC field,

$$I(V, A_0, \mathbf{n}) = e \sum_{\bar{n}} P(\bar{n}) \left[\bar{\Gamma}_k^+(\Delta E_k^+(\bar{n}, V), A_0, \mathbf{n}) - \bar{\Gamma}_k^-(\Delta E_k^-(\bar{n}, V), A_0, \mathbf{n}) \right]. \quad (1.9)$$

We will consider the transport voltage V as the input variable and the current I as the output function in implementing neuromorphic computation. For a two-dimensional quantum-dot array with K rows, we can readily generalize the description given here to consider K input voltages V_k and output currents $I_k(V_k, A_0, \mathbf{n})$. This function of K inputs and K outputs is controllable through the parameters of the external,

alternating field, A_0 and v , by minimizing the error function \mathcal{E} , defined as the squared difference between the observed currents, I_k , and the expected currents, I_k^* ,

$$\mathcal{E} \equiv \frac{1}{K} \sum_{k=1}^K [I_k(V_k, A_0, \mathbf{v}) - I_k^*]^2. \quad (1.10)$$

If a larger number of controls are necessary, then a multicomponent AC field may be implemented as the global control, rather than a monochromatic external-driving field.

The pattern recognition scheme can now readily be implemented using the following method. We assume that two sets of K vectors are used for training. They are stored as rows of two matrices $\mathbf{\Omega}_{KI}$ and \mathbf{R}_{KO} respectively, which represent the input signal patterns and the target outputs. For convenience, the matrix dimensions are explicitly indicated as subscripts. The number of columns of each matrix (I for input, O for output) equals the number of nodes of the corresponding processing layer in the quantum dot-array. Since typically $K \gg I$, a preprocessing step is used [10]. Specifically, two successive *nonlinear* transformations map $\mathbf{\Omega}_{KI}$ into \mathbf{H}_{KK} , a nonsingular $K \times K$ presynaptic matrix, which constitutes the actual input into the array. We also decouple the nonlinearity of the transfer function at the output layer of the neural net from the linear interlayer pattern propagation mediated by the synaptic weights \mathbf{W}_{KO} . This transformation is used to compute the postsynaptic input to the output layer of the neural net as a $K \times O$ rectangular matrix. Since the latter is connected via a bijective sigmoid mapping to the output training examples, the synaptic interconnection matrices \mathbf{W}_{KO} can be determined. In simulation on a conventional computer, this can be done exactly by solving a system of linear equations using singular value decomposition techniques. On nanoelectronic hardware, this will be achieved by directly optimizing the error function in Eq. (1.10) in terms of the parameters of the external field, A_0 and v .

In this minimization process, we can directly account for uncertainties to obtain best estimates for the device parameters and responses of interest. For example, nominal values for the elements of the capacitance matrix will be computed from “first-principles” simulations of the metal clusters and substrate via density-functional-theory-based molecular dynamics [36] and the current through the device will be computed via numerical solutions to the master equation [14,15]. To obtain best estimates for critical parameters (e.g., A_0 and v), we must consistently combine computational results and experimental measurements. We achieve this by optimizing a generalized Bayesian loss function that simultaneously minimizes the differences between the best estimate responses and the measured responses on one hand, and the best estimate and calculated parameters on the other hand. Our optimization process uses the inverse of a generalized total covariance matrix as the natural metric of the calculational manifold in conjunction with response sensitivities to all parameters [37].

ACKNOWLEDGMENTS

Research partially sponsored by the Engineering Research Program of the Office of Basic Energy Sciences, U.S. DOE, and partially by the Laboratory Directed Research and Development Program of Oak Ridge National Laboratory (ORNL), managed by UT-Battelle, LLC for the U. S. DOE under Contract No. DE-AC05-00OR22725.

REFERENCES

1. M. ZHAO and R.M. CROOKS, “Intradendrimer Exchange of Metal Nanoparticles,” *Chem. Mater.* **11**, 3379 (1999).
2. J. CHEN *et al.*, “Synthesis from DNA of a Molecule with the Connectivity of a Cube,” *Nature*, **350**, 631 (1991).
3. J. QI, *et al.*, “Ligation of Triangles Built from Bulged 3-Arm DNA Branched Junctions,” *J. Am. Chem. Soc.* **118**, 6121 (1996).
4. Y. ZHANG and N.C. SEEMAN, “Construction of a DNA-Truncated Octahedron,” *J. Am. Chem. Soc.*, **116**, 1661 (1994).
5. X. LI, X. YANG, J. QI, and N.C. SEEMAN, “Antiparallel DNA Double Crossover Molecules as Components for Nanoconstruction,” *J. Am. Chem. Soc.* **118**, 6131 (1996).
6. E. WINFREE, *et al.*, “Design and Self-Assembly of Two-Dimensional DNA Crystals,” *Nature* **394**, 539, (1998).
7. J.E. MUELLER, *et al.*, “Design and Synthesis of a Knot from Single-Stranded-DNA,” *J. Am. Chem. Soc.* **113**, 6306, (1991).

- Jap. Jour. Applied Phys.*, **35**(6), 3350-3362 (1996).
32. J.A MELSEN, *et al.*, "Coulomb Blockade Threshold in Inhomogeneous One-Dimensional Arrays of Tunnel Junctions," *Phys. Rev. B* **55**, 10638 (1997).
 33. L. P. KOUWENHOVEN *et al.*, "Quantized Current in a Quantum-Dot Turnstile Using Oscillating Tunnel Barriers", *Phys. Rev. Lett.* **67**, 1626-1629 (1991).
 34. M. N. WYBOURNE *et al.*, "Coulomb-Blockade Dominated Transport in Patterned Gold-Cluster Structures", *Jap. Jour. Appl. Phys.*, **36**, 7796 (1997).
 35. T. OOSTERKAMP *et al.*, "Photon Assisted Tunneling in Quantum Dots", *arXiv:cond-mat/9904359*, Los Alamos National Laboratory (26 April 1999).
 36. P. BALLONE and W. ANDREONI, "Density Functional Theory and Car-Parrinello Molecule Dynamics for Metal Clusters," in *Metal Clusters*, Ed. W. Ekardt, (Wiley, 1999).
 37. J. BARHEN and V. PROTOPOPESCU, "Ultrafast Neural Network Training for Robot Learning from Uncertain Data", in *Distributed Autonomous Robotic Systems* L. Parker ed., Springer (in press, 2000).